Green Chemistry

PAPER

View Article Online
View Journal | View Issue

Cite this: *Green Chem.*, 2022, **24**, 2795

Integrating lignin depolymerization with microbial funneling processes using agronomically relevant feedstocks†

Jose M. Perez, ‡[a,b,c] Canan Sener, ‡[b,c] Shamik Misra, ‡[c,d] German E. Umana,[a,b,c] Jason Coplien,[b,c] Dennis Haak,[b,c] Yanding Li,[b,c] Christos T. Maravelias,[d,e] Steven D. Karlen,[b,c] John Ralph,[b,c,f] Timothy J. Donohue[b,c,g] and Daniel R. Noguera *[a,b,c]

The economic feasibility of the lignocellulosic biomass refinery requires the valorization of lignin in addition to its polysaccharide fraction. One promising approach is the combination of chemical methods for lignin fractionation and depolymerization with microbial funneling of the resulting phenolic monomers into valuable chemicals. In this work, we explored the integration of γ-valerolactone (GVL) for biomass pretreatment, catalytic hydrogenolysis for lignin depolymerization, and microbial funneling to 2-pyrone-4,6-dicarboxylic acid (PDC) by the engineered bacterium *Novosphingobium aromaticivorans* strain PDC. We first investigated the microbial PDC production feasibility from common phenolic compounds previously identified in lignin hydrogenolysis products. Next, we studied the PDC production potential from maple, poplar, sorghum, and switchgrass using the proposed integrated pipeline and, finally, we performed a technoeconomic analysis (TEA) of the system to identify parameters that affect its economic feasibility. We found that *N. aromaticivorans* strain PDC is able to produce PDC from phenolic compounds with propanol, methyl, or methyl ester sidechains. Using Pd/C as a catalyst for hydrogenolysis to favor the production of these phenolics from lignin extracted with the GVL process, we obtained microbial PDC production yields of 88, 139, 103, and 79 g PDC per kg lignin from maple, poplar, sorghum, and switchgrass, respectively. Using these yields, we estimated a baseline minimum selling price of $12.10 per kg of purified PDC, and identified options to further improve the integrated pipeline.

Received 30th September 2021,
Accepted 18th February 2022

DOI: 10.1039/d1gc03592d

rsc.li/greenchem

Introduction

Plant biomass is a promising and abundant raw material for the production of liquid fuels and commodity chemicals within the context of a sustainable and carbon-neutral economy.[1] Plant biomass is primarily composed of cell-walls that consist of the polysaccharides, cellulose and hemicelluloses, and the phenolic heteropolymer lignin. Whereas numerous techniques have been developed to valorize the sugar fraction, the lignin fraction has for the most part remained an untapped resource. This is due to challenges derived from its heterogeneity and natural recalcitrance to many deconstruction methods. Combined with lignin's tendency to condense under classical pulping and harsh pretreatment conditions, the utilization of the lignin fraction has been mostly limited to a low-value source of process heat and energy,[2] or as filler material in construction applications.[3] The economic feasibility of biorefineries based on plant biomass depends on efficiently utilizing as much of this material as possible as a source of valuable products.[4–6] Additional efforts are therefore necessary to develop techniques capable of economically upconverting the underutilized lignin and phenolic fractions to commodity chemicals.

One approach to valorize lignin is to combine chemical depolymerization to generate an array of depolymerized lignin products with microbial funneling of those mixtures into a

[a]*Department of Civil and Environmental Engineering, University of Wisconsin-Madison, Madison, Wisconsin 53706, USA. E-mail: noguera@engr.wisc.edu*
[b]*Wisconsin Energy Institute, University of Wisconsin-Madison, Madison, Wisconsin 53726, USA*
[c]*Great Lakes Bioenergy Research Center, University of Wisconsin-Madison, Madison, Wisconsin 53726, USA*
[d]*Andlinger Center for Energy and the Environment, Princeton University, Princeton, NJ, 08544, USA*
[e]*Department of Chemical and Biological Engineering, Princeton University, Princeton, New Jersey 08544, USA*
[f]*Department of Biochemistry, University of Wisconsin-Madison, Madison, Wisconsin 53726, USA*
[g]*Department of Bacteriology, University of Wisconsin-Madison, Madison, Wisconsin 53706, USA*
†Electronic supplementary information (ESI) available. See DOI: 10.1039/d1gc03592d
‡These authors equally contributed to this work.

single valuable product.[7] One of the target products of biological funneling is 2-pyrone-4,6-dicarboxylic acid (PDC), an intermediate in the metabolism of lignocellulose-derived aromatic compounds by some bacteria.[8–10] PDC could be used as a precursor to bioplastics,[11] rubber, and epoxy adhesives,[12] or as a chemical for water reclamation by selectively removing radioactive cesium from ocean water.[13] PDC can be biologically produced with engineered microbes from single aromatic compounds,[9,14,15] plant biomass extracts,[16] industrial lignin extracts,[16,17] and non-lignin-derived substrates such as glucose.[18] Reports of microbial funneling to PDC have highlighted the diversity of phenolic streams derived from biomass processes that could be utilized; these include extracts from kraft pulping, nitrobenzene oxidation[16] or other oxidative lignin depolymerization,[9] and lignosulfonates from sulfite pulping.[17]

Various lignin depolymerization techniques are currently under investigation, most of which use heterogenous catalysts under either reductive or oxidative conditions.[19–21] Many of these catalytic processes target cleavage of the abundant β-aryl-ether bonds; the efficiency of depolymerization to aromatic monomers is therefore proportional to the fraction of the inter-unit linkages that are β-aryl ethers, which in turn is correlated to the source and quality of the lignin. Native-like lignins produce a higher monomer aromatic yield,[6,22] whereas highly condensed lignins (*e.g.*, kraft lignin) with few surviving β-aryl-ether bonds produce few monomers. We have previously demonstrated that the high-quality lignin stream produced by the γ-valerolactone (GVL) process is suitable for catalytic hydrogenolysis to phenolic monomers.[23] The GVL process is an acidic organosolv technique that utilizes a mixture of 80% GVL and 20% water with 100–500 mM sulfuric acid. A biorefinery based on the GVL process could produce a product portfolio comprising a dissolvable pulp, furfural, and a high-quality lignin stream.[24] Benefits of the GVL process over other biomass deconstruction strategies include the ability to process different types of biomass (*e.g.*, hardwoods, softwoods, and grasses) in a biomass-agnostic manner and, when operated to include a high-temperature stage, the process can depolymerize cellulose and hemicelluloses into monomeric sugars without the need for enzymatic hydrolysis.[25]

We are interested in expanding the GVL-based deconstruction platform to include a process for heterogenous catalytic depolymerization of the high-quality lignin stream and microbial funneling of the resulting phenolic monomers to generate lignin-derived coproducts. In previous work, we showed that an engineered strain of *Novosphingobium aromaticivorans* DSM12444 (strain PDC) was able to produce PDC from a multitude of aromatic compounds commonly found after oxidative lignin depolymerization and demonstrated its application with oxidatively depolymerized lignin from poplar.[9] We now look to expand the set of depolymerization processes to include reductive depolymerization, which produces a different set of products that have fewer degrees of unsaturation and lower oxygen content than the products from oxidative processes. The reductive depolymerization products have not been tested as substrates for microbial production of PDC. Catalytic hydrogenolysis, or reductive catalytic fractionation (RCF), is a reductive processes that produces high yields of phenolic monomers (typically 20–60% in hardwoods) and oligomers under many different catalytic conditions.[20,21] When performed under milder conditions, the catalyst cleaves the aryl-ether bonds and saturates non-aromatic double bonds producing a viscous oil with mildly complex chemical composition.[20,26] Under harsher conditions the catalyst can reduce all the double bonds (including those in aromatic rings), deoxygenate the lignin, and cleave some C–C bonds generating light hydrocarbons (similar to those from hydrocarbon cracking).[27] Catalytic depolymerization conditions utilizing Pd/C, Ni/C, Ni/Al_2O_3, Rh/C, and other heterogenous catalysts can be designed to favor products that retain the main syringyl (S), guaiacyl (G), or *p*-hydroxyphenyl (H) phenolic substructures with propanol as the sidechain.[21,28–33] Under slightly different conditions these same catalysts, as well as others (*e.g.*, solid-supported Ru, Pt, Zn, and Cu catalysts) can be designed to favor propyl sidechains or even the fully saturated propyl-cyclohexanes.[19,20]

In this study, we expanded our previous work on integrating the GVL-biorefinery producing lignin, furfural, and dissolving pulp[24] with lignin hydrogenolysis[23] to test biological funneling of the reductive hydrogenolysis product mixture in a biomass-to-PDC pipeline (Fig. 1). With the large array of possible aromatic monomers that can be produced by hydrogenolysis, we first evaluated which compounds could be used by the PDC-producing *N. aromaticivorans* strain.[9] With this new knowledge, we chose a catalyst (Pd/C) that favors generating product mixtures predicted to be converted to PDC at high yield by an engineered microbe. We applied these pipeline conditions to four industrially-relevant biofuel feedstocks that represent both hardwoods and grasses, namely hard maple, poplar, energy sorghum, and switchgrass, and demonstrated a high efficiency for conversion of reductive hydrogenolysis products to PDC. These results expand the repertoire of plant-derived aromatic compounds that can be used in microbial funneling by *N. aromaticivorans*. To our knowledge, this is the first report on biological funneling, into a single product, of H-, G-, and S-type aromatic monomers obtained *via* reductive lignin depolymerization. We then applied the knowledge gained through experimental observations into a technoeconomic analysis (TEA) to identify unit processes in this pipeline with the greatest impact on the minimum selling price (MSP) of a PDC salt product. This comparative evaluation of product yields from different feedstocks offers important new observations needed to optimize the feasibility of a biomass-to-product pipeline that uses GVL deconstruction followed by lignin depolymerization by hydrogenolysis and biological funneling to PDC.

Results

Conversion of aromatic hydrogenolysis products to PDC

Lignin hydrogenolysis performed under mild conditions produces several aromatic compounds that retain the methoxy

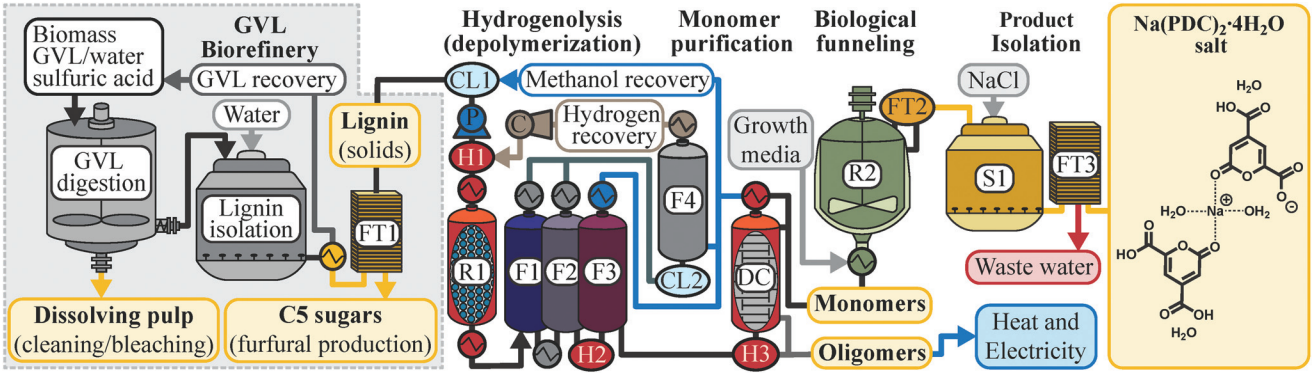

Fig. 1 Schematics of a GVL-biorefinery producing furfural, high-quality lignin, and dissolving pulp, in which the lignin stream is up-converted to PDC using a combination of lignin hydrogenolysis and biological funneling. R1: hydrogenolysis reactor; R2: microbial transformation; F1: flash column to step down from 65 bar to 1 bar; F2: flash column to step temperature down to 75 °C; F3: flash column to recover >99% methanol; F4: flash column to separate recovered hydrogen and methanol; DC: distillation column to separate phenolic monomers from oligomers; S1: settling tank for isolation of $Na(PDC)_2$ salt; P: pump for methanol-lignin feed stream; C: hydrogen compressor to 65 bar; H1: heater for hydrogenolysis feed; H2: heater for methanol recovery; H3: heater for phenolic monomer distillation; FT1, FT2, FT3: filters; CL1 and CL2: chillers.

groups of the phenolic subunits and have different sidechains. The composition of the dominant sidechains are tuned by the reaction conditions (*e.g.*, catalyst type and loading, solvent, pressure, lignin concentration, reaction temperature, and residence time).[19,20] Under mild conditions using Pd/C as the catalyst, the major phenolic monomer products of hydrogenolysis are phenolic S or G units with 3-propanol [dihydrosinapyl alcohol (DSA) and dihydroconiferyl alcohol (DCA)] or propyl sidechains [propylsyringol (PS) and propylguaiacol (PG)]. When the lignin is from *Populus* or *Salix* hardwoods (*e.g.*, poplar, aspen, and willow) the lignin-bound *p*-hydroxybenzoate is released by transesterification to form *p*-hydroxybenzoic acid methyl ester (Me-*p*HBA, methyl *p*-hydroxybenzoate) as one of the major hydrogenolysis products. Similarly, grass-derived lignins (*e.g.*, from sorghum or switchgrass) contain lignin-bound *p*-coumarate and ferulate esters, both of which undergo transesterification to the methyl esters and hydrogenation of the vinyl group to give 7,8-dihydro-*p*-coumaric acid methyl ester (Me-DH*p*CA) and 7,8-dihydroferulic acid methyl ester (Me-DHFA), which are also major monomeric products from these depolymerized feedstocks.[20] As the microbial transformation and fate of these products is largely unknown, we tested the transformation and PDC yield when the individual aromatic compounds were fed to our engineered PDC-producing strain in minimal medium containing glucose (Fig. 2, Table 1 and Table S1†). Glucose was used in these experiments to promote cell growth because the metabolism of aromatics is blocked downstream of PDC.[9] We also tested PDC production from other aromatic compounds known to be minor products of hydrogenolysis, such as the phenolic S and G units with a methyl [methylsyringol (MS) and methylguaiacol (MG)] or ethyl [ethylsyringol (ES) and ethylguaiacol (EG)] sidechains, as well as the parent phenolics lacking a sidechain, guaiacol, and syringol (Fig. S1† and Table 1).

All the major hydrogenolysis products (Fig. 2) were consumed by *N. aromaticivorans* strain PDC, but not all of them led to accumulation of PDC. PDC accumulation was observed from DSA, DCA, Me-DHFA, Me-DH*p*CA, and Me-*p*HBA (Fig. 2, panels A to E), whereas growth in the presence of the aromatics PS and PG did not yield significant PDC accumulation (Fig. 2, panels F and G). Instead, we observed accumulation of extracellular metabolites (Fig. S2†) that were identified to be the products of sidechain oxidation, primarily 4-hydroxy-3-methoxyphenylpropanone (GPO) and 3,5-dimethoxy-4-hydroxyphenylpropanone (SPO). The rates at which these aromatic substrates were consumed varied but, by the end of the experiments (19 or 24 h), only PG and Me-*p*HBA were detectable in the culture medium. The PDC yield from the aromatics that were transformed to PDC varied from ~50–100%, with highest yields observed for compound with zero or one methoxy group (Me-DHFA, Me-DH*p*CA, Me-*p*HBA), whereas the lower yields were obtained with DSA that contains two aromatic methoxy groups (Table 1).

To evaluate whether GPO and SPO were transformed by *N. aromaticivorans* strain PDC, cultures in minimal media supplemented with glucose and either GPO or SPO were tested (Fig. S3†). These experiments showed poor utilization of the aromatic substrates and only traces of PDC production, indicating that GPO and SPO are byproducts not further transformed by *N. aromaticivorans*.

Among the minor aromatic hydrogenolysis products tested (Fig. S1†), the cultures supplemented with ES and EG showed consumption of the aromatic compound, but instead of forming PDC the microbes produced acetosyringone (AS) from ES and acetovanillone (AV, apocynin, acetoguaiacone) from EG (Fig. S4†). Bacterial growth experiments with *N. aromaticivorans* strain PDC cultured in media supplemented with glucose and either AS or AV showed minimal removal of the aromatic substrates and only traces of PDC accumulation (Fig. S5†). MS and MG were partially transformed to PDC (Fig. S1,† panels C and D), with PDC yields of 28% and 66%, respectively (Table 1). In cultures supplemented with syringol,

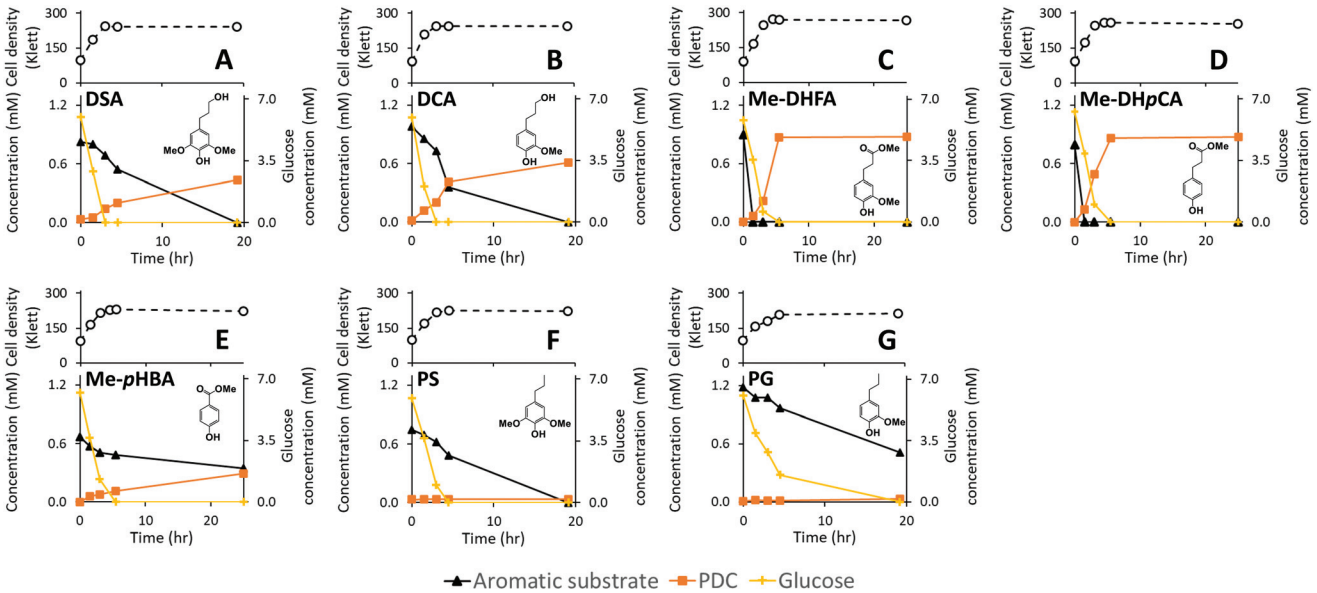

Fig. 2 Probing the ability of *N. aromaticivorans* strain PDC cultures to convert the major hydrogenolysis products to PDC in minimal media supplemented with glucose plus the indicated aromatic compound. Cell density and extracellular metabolite concentration of cultures supplemented with 7,8-dihydrosinapyl alcohol (DSA) (A), 7,8-dihydroconiferyl alcohol (DCA) (B), 7,8-dihydroferulic acid methyl ester (Me-DHFA) (C), 7,8-dihydro-*p*-coumaric acid methyl ester (Me-DH*p*CA) (D), *p*-hydroxybenzoic acid methyl ester (Me-*p*HBA) (E), propylsyringol (PS, syringylpropane) (F), and propylguaiacol (PG, guaiacylpropane) (G). Values correspond to the average of three biological replicates.

Table 1 Yield of PDC (mol) at 19–24 h reaction time from the aromatic substrates screened in this study. Standard error was determined from $n = 3$ technical replicates

	Compound	*R*	PDC molar yield (%)
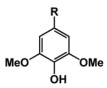	Propylsyringol (PS)		0.3% ± 0.5%
	7,8-Dihydrosinapyl alcohol (DSA)		48.6% ± 3.2%
	Ethylsyringol (ES)		0.9% ± 0.0%
	Methylsyringol (MS)		28.0% ± 2.7%
	Syringol	H	5.4% ± 3.5%
	Propylguaiacol (PG)		3.5% ± 1.1%
	7,8-Dihydroconiferyl alcohol (DCA)		60.5% ± 1.4%
	7,8-Dihydroferulic acid methyl ester (Me-DHFA)		97.9% ± 0.3%
	Ethylguaiacol (EG)		1.7% ± 1.1%
	Methylguaiacol (MG)		66.3% ± 2.6%
	Guaiacol	H	2.3% ± 1.6%
	*p*-Hydroxybenzoic acid methyl ester (Me-*p*HBA)		91.6% ± 6.2%
	7,8-Dihydro-*p*-coumaric acid methyl ester (Me-DH*p*CA)		*Quant.*

a small reduction in its concentration was observed while there was glucose present and cells were growing (Fig. S1E†). On the other hand, cultures supplemented with guaiacol showed a consumption of the aromatic substrate even after all glucose was consumed and the compound was completely degraded with no extracellular aromatic metabolite accumulation (Fig. S1F†).

In sum, the experiments with pure compounds that are either products of hydrogenolysis or byproducts accumulated during microbial transformation helped identify those aromatic compounds leading to PDC production (DSA, DCA, Me-DHFA, Me-DH*p*CA, Me-*p*HBA, MS, MG), those degraded by pathways that do not have PDC as an intermediate metabolite (PS, PG, ES, EG, guaiacol), and those not transformed by *N. aromaticivorans* strain PDC (GPO, SPO, AS, AV, syringol).

Lignin isolation and depolymerization

The use of purified compounds as substrates showed that the *N. aromaticivorans* PDC strain can produce PDC from aromatics containing propanol, methyl, or methyl ester side-

chains and does not produce PDC from aromatics containing a propyl or ethyl sidechain, nor from aromatics without an alkyl sidechain. Scanning across the literature for the various catalysts, Pd/C,[29,34–36] Rh/C,[37] Ni/C,[35] and Ni/Al_2O_3,[33,35] the Pd/C catalyst pair has advantages of being fairly air stable and produces the highest propanol selectivity over a range of reaction conditions.[19,31] We therefore selected commercially available Pd/C catalyst for the following hydrogenolysis experiments. To ensure a high quality (native-like) isolated lignin, we performed the GVL process under the mild conditions reported to minimize lignin degradation and condensation,[23] although this resulted in lower lignin extraction efficiencies compared to harsher conditions that are required to liquefy the cellulose fraction of the biomass.[23]

A wide array of solvents has been shown to be compatible with hydrogenolysis and it is known that the choice of solvent can alter product distributions.[19] As a starting point for integrating hydrogenolysis with microbial funneling, we chose to use methanol as a solvent due to its low boiling point, low cost, and relatively low toxicity. Methanol also helps to pull the hydrophobic hydrogenolysis products into the aqueous media. The Pd/C catalyst was used as received from the manufacturer to provide a baseline for the process. We selected four plant species as biomass sources, namely hard maple, poplar, energy sorghum, and switchgrass. The maple is representative of most hardwood species and has a lignin composition of mostly S and G units.[38] HSQC NMR analysis of the GVL-extracted maple lignin indicated an S/G ratio of 1.97 (66 : 34 S : G), an S*/S ratio of 0.45, which is indicative of some degree of lignin condensation, and consisting of 58% β-ether, 21% phenylcoumaran, and 21% resinol units (Table 2 and Fig. S6A†). Poplar (and all *Populus* species) are hardwoods characterized by the presence of *p*-hydroxybenzoate pendent groups on their lignin *S*-units.[39–44] The poplar used in this study, a *Populus maximowiczii* × *nigra* hybrid (NM6), has been reported[45] to have an S/G ratio of 1.5 (60 : 40 S : G). NMR analysis of poplar lignin extracted using the GVL process showed a S/G ratio of 2.15 (68 : 32 S/G), an S*/S ratio of 0.35, and estimated to contain relative levels of 77% β-ether, 16% phenylcoumaran, and 8% resinol units (Table 2, Fig. S6B†). Sorghum and switchgrass are both grasses that are known to process relatively easily due to arabinoxylan hemicelluloses that contain high levels of arabinose-bound ferulate cross-linkages to strengthen the walls with lower lignin levels.[46] The lignin composition of the two grasses is different, with sorghum having a higher S content and an S/G ratio of 0.93 (48 : 52 S : G) and an S*/S ratio of 0.28, whereas switchgrass is higher in G content with an S/G ratio of 0.71 (42 : 58 S : G) and an S*/S ratio of 0.34 (Table 2). The changes in the unit-type composition reflects the difference in S/G ratio, with sorghum having 66% β-ether, 22% phenylcoumaran, and 12% resinol units, whereas switchgrass was comprised of 61% β-ether, 26% phenylcoumaran, and 13% resinol (Table 2, Fig. S8C and D†).

Applying the lignin extraction process[23] described in the Materials and methods section to the four feedstocks resulted in isolated lignins with yields of 15% (maple), 22% (poplar),

Table 2 Characterization of the lignin and hydrogenolysis product mixtures from the four representative biomasses, maple (S/G hardwood), poplar (S/G hardwood with *p*-hydroxybenzoate (*p*HBA) esters), and the grasses sorghum and switchgrass [with different levels of *p*-coumarate (*p*CA) and ferulate (FA) esters]. Standard error was determined from n = 3 technical replicates

Characteristic	Maple	Poplar	Sorghum	Switchgrass
Lignin content				
wt% Klason lignin	25%	24%	16%	19%
wt% of Klason lignin that was extracted with GVL process	15%	22%	35%	41%
NMR analysis of the GVL-extracted lignins				
S : G[b]	66 : 34	68 : 32	48 : 52	42 : 58
S/G ratio	1.97	2.15	0.93	0.71
S*/S ratio (indication of lignin condensation)[c]	0.45	0.35	0.28	0.34
Cinnamaldehyde[b]	2%	3%	2%	2%
Tricin[b]	0%	0%	15%	4%
p-Hydroxybenzoate	0%	26%	0%	0%
p-Coumarate	0%	0%	47%	17%
Ferulate	0%	0%	3%	3%
Sidechains: β-O-4 :β-5 : β–β (β-ether : phenylcoumaran : resinol)[d]	58 : 21 : 21	77 : 16 : 8	66 : 22 : 12	61 : 26 : 13
Distribution of monomers after hydrogenolysis (mol%)[a]				
Propanol sidechain	75% (76%)	63% (72%)	23% (53%)	36% (60%)
Propyl sidechain	8% (8%)	19% (22%)	15% (33%)	15% (24%)
Ethyl sidechain	5% (5%)	2% (2%)	3% (7%)	5% (8%)
Methyl sidechain	7% (8%)	3% (3%)	2% (5%)	3% (6%)
Phenols (no sidechain)	3% (3%)	1% (1%)	1% (2%)	1% (2%)
Methyl esters (Me-*p*HBA, Me-DH*p*CA, Me-DHFA)	2%	12%	56%	40%
Extracted Lignin				
Monomers (wt%, extracted lignin basis)	9.0 ± 0.2%	19.9 ± 0.9%	11.7 ± 0.2%	8.6 ± 0.1%
Methyl ester monomers (wt%, extracted lignin basis)	0.1 ± 0.1%	1.7 ± 0.1%	6.3 ± 0.2%	6.3 ± 0.2%

[a] Values in parenthesis correspond to the mol% of the total monolignol-derived monomers (excluding esters). [b] Values reported on a $[0.5 \times (S_{2/6} + S'_{2/6}) + G_2 = 100]$ basis; as terminal units and pendent groups these components are over-represented in the NMR data.[47,48] [c] As the lignin becomes more condensed, the correlation signal from condensed *S*-units (*S**) increases in abundance *vs.* those from the *S*-units ($S_{2/6} + S'_{2/6}$). [d] Values reported on a $[A_\alpha + B_\alpha + 0.5 \times (C_\alpha + C'_\alpha) = 100]$ basis.

35% (sorghum), and 41% (switchgrass), with respect to the Klason lignin values that are considered to be the best measurement of the total lignin content of biomass. Experiments with these four feedstocks provide insight into the efficiency of isolating native-like lignins and how lignin composition alters the downstream processes relating to hydrogenolysis monomer yield and microbial conversion to PDC, as discussed below.

The composition of the hydrogenolysis oil formed under the hydrogenolytic reaction conditions used was analyzed *via* GC/FID. As expected from previous studies,[19,34] the aromatic monomer product distribution heavily favored the production of propanol over the propyl or truncated (ethyl or methyl) sidechains, as shown in Table 2; Table S2† shows the product distribution of individual compounds. The maple and poplar had 76% and 72% of the monolignol-derived monomers (excluding products from ester units) as aryl-propanols, whereas the grasses released a lower relative level of propanols, with sorghum at 53% and switchgrass at 60% (Table 2). These differences in propanol *vs.* propyl/truncated sidechains are masked somewhat by the amount of released esters (Me-*p*HBA, Me-DH*p*CA, Me-DHFA). In the case of poplar, *p*HBA comprised 12% of the quantified monomers (monolignol-derived + ester-derived units). For sorghum and switchgrass, the sums of *p*CA and FA were 56% and 40% of the quantified monomers. There is some correlation between ester release (content) and the observed decrease in selectivity toward aryl-propanol over aryl-propyl products, presumably a result of addition of H_2 across the C_γ–O bond releasing the free carboxylic acid. Overall, the fraction of aromatic monomers expected to result in PDC production by the engineered *N. aromaticivorans* strain, based on the experiments with individual compounds (*i.e.*, sum of monomers with propanol and methyl sidechains or methyl esters in Table 2) was 84%, 78%, 81%, and 81% for maple, poplar, sorghum, and switchgrass, respectively.

Production of PDC from lignin hydrogenolysis products

The hydrogenolysis oil was diluted in minimal media (see Materials and methods) that was supplemented with glucose to provide a known and constant carbon source for bacterial growth. This medium was mixed with a culture of the PDC strain at a 1 : 1 v/v ratio to initiate the growth experiments. An abiotic control was prepared by mixing the same glucose-supplemented medium containing diluted hydrogenolysis oil with sterile medium at a 1 : 1 v/v ratio. The composition of the media in the different cultures and the abiotic control was monitored during the experiments using HPLC/MS.

In most cultures, the aromatic compounds were consumed within the first 8 hours (Fig. 3 and Table S3†). The cultures used in testing the transformation of depolymerized lignin from poplar (Fig. 3B) produced the most PDC but they took longer to completely consume the monitored aromatic compounds, possibly because they contained the highest initial concentrations of aromatic monomers. In all samples inoculated with bacteria, PDC accumulated in the culture medium, reaching maximal concentrations of 0.12 ± 0.01 mM, 0.19 ± 0.01 mM, 0.14 ± 0.01 mM, and 0.11 ± 0.01 mM for maple, poplar, sorghum, and switchgrass, respectively (Fig. 3). The calculated yields of PDC in these cultures were 88.4 ± 0.1, 139.1 ± 0.3, 103.3 ± 4.6, and 79.2 ± 0.4 g PDC per kg lignin for maple, poplar, sorghum, and switchgrass, respectively (Table 3). When product yields were calculated per kg of whole cell wall (WCW), which accounts for efficiencies in lignin extraction, hydrogenolysis, and microbial conversion combined, the observed PDC yields were 3.04 ± 0.25, 7.52 ± 0.02,

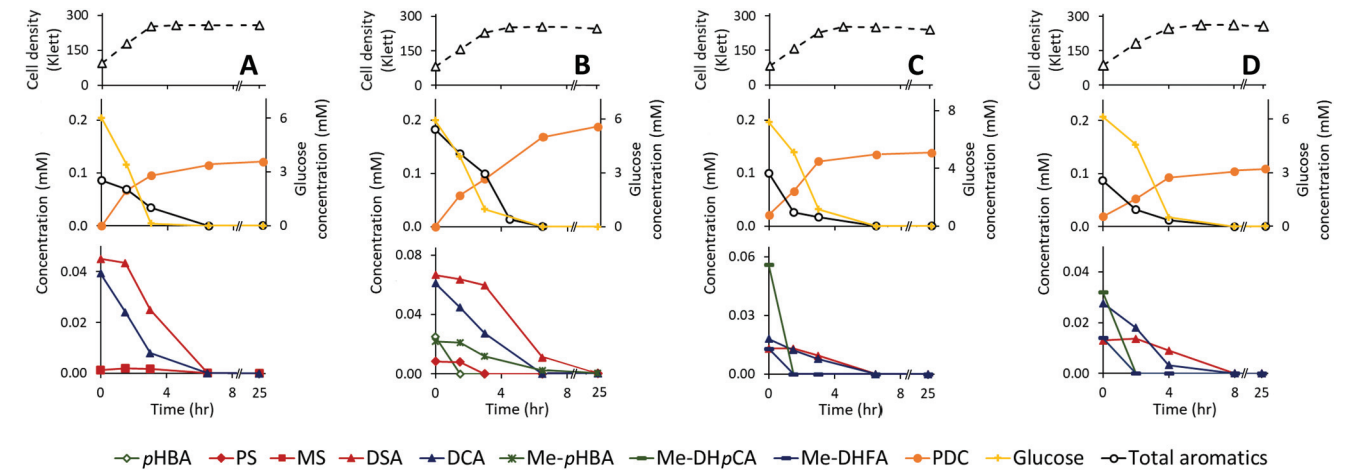

Fig. 3 Representative *N. aromaticivorans* strain PDC cultures grown in minimal media supplemented with glucose and depolymerized lignin from maple (A), poplar (B), sorghum (C), and switchgrass (D). (Top row of plots) cell density, (middle row of plots) glucose, total aromatics and PDC production, (bottom row of plots) concentration of primary monophenolic products from hydrogenolysis present in the culture media. Abbreviations: *p*-hydroxybenzoic acid (*p*HBA), propylsyringol (PS), methylsyringol (MS), 7,8-dihydrosinapyl alcohol (DSA), 7,8-dihydroconiferyl alcohol (DCA), *p*-hydroxybenzoic acid methyl ester (Me-*p*HBA), 7,8-dihydro-*p*-coumaric acid methyl ester (Me-DH*p*CA), 7,8-dihydroferulic acid methyl ester (Me-DHFA), and 2-pyrone-4,6-dicarboxylic acid (PDC). Each data point corresponds to the average of three biological replicates using the lignin hydrogenolysis products from one of three depolymerization reactions.

Table 3 PDC produced by *N. aromaticivorans* strain PDC from depolymerized lignin obtained from maple, poplar, sorghum, and switchgrass. Standard error was determined from n = 3 technical replicates

PDC yield	Maple	Poplar	Sorghum	Switchgrass
g PDC per kg lignin	88.4 ± 0.1	139.1 ± 0.3	103.3 ± 4.6	79.2 ± 0.4
g PDC per kg WCW	3.04 ± 0.25	7.52 ± 0.02	5.78 ± 0.26	6.29 ± 0.03
wt% PDC from lignin	8.8%	13.9%	10.3%	7.9%
mol% PDC from total aromatics measured in depolymerized lignin	108.9%	71.1%	90.7%	100.5%
Predicted PDC yield based on monomers quantified in the hydrogenolysis product mix and the experimental yields obtained for individual compounds (g PDC per kg lignin)	38.0	95.9	85.3	53.3
Predicted PDC yield based on monomers quantified in the hydrogenolysis product, assuming a stoichiometric yield of PDC from each convertible monomer (g PDC per kg lignin)	70.4	159.3	99.3	68.8

5.78 ± 0.26, and 6.29 ± 0.03 g PDC per kg WCW for maple, poplar, sorghum, and switchgrass, respectively (Table 3).

On a molar basis, calculated from the quantification of the aromatic monomers detected at the beginning of the incubation (Table S3†) and the final concentration of PDC, the PDC yields were 109%, 71%, 91%, and 100% for maple, poplar, sorghum, and switchgrass, respectively (Table 3).

On a mass basis (g PDC per kg lignin), the observed PDC yields from the deconstructed lignins were higher than those predicted based on the concentration of aromatic monomers measured in the hydrogenolysis products and the observed PDC yield from each of the purified aromatics (Table 3). In the case of maple and switchgrass, the observed yields are higher than predictions that even assume stoichiometric yield of PDC from each convertible monomer (Table 3). One interpretation of this result is that the hydrogenolysis product contains as yet unidentified aromatics or other compounds that are metabolized by *N. aromaticivorans* and contribute to PDC accumulation (Table 3).

Technoeconomic analysis

Based on this experimental data, an integrated lignin-to-PDC process was designed, and a process simulation model was developed to identify the areas requiring the most improvement and to determine an approximate minimum selling price (MSP) for the PDC. The designed process consisted of five main sections (Fig. 4 and Fig. S7†): (1) catalytic depolymerization of lignin (hydrogenolysis); (2) separation of phenolic monomers from oligomers; (3) biological funneling of phenolic monomers to PDC; (4) isolation of the PDC as the sodium salt $Na(PDC)_2$; and (5) generation of process heat and electricity. The economic parameters and other assumptions are summarized in Table S4,† whereas the key data used as the baseline for the refinery design are reported in Table 4. Note that, although the lignin isolation (GVL-biorefinery) section is shown in Fig. 1, we modeled the lignin to PDC process that starts with lignin as the feedstock. To estimate the feedstock (lignin) cost, we used the process model and parameters provided by Alonso *et al.*,[24] who studied a GVL-based biorefinery.

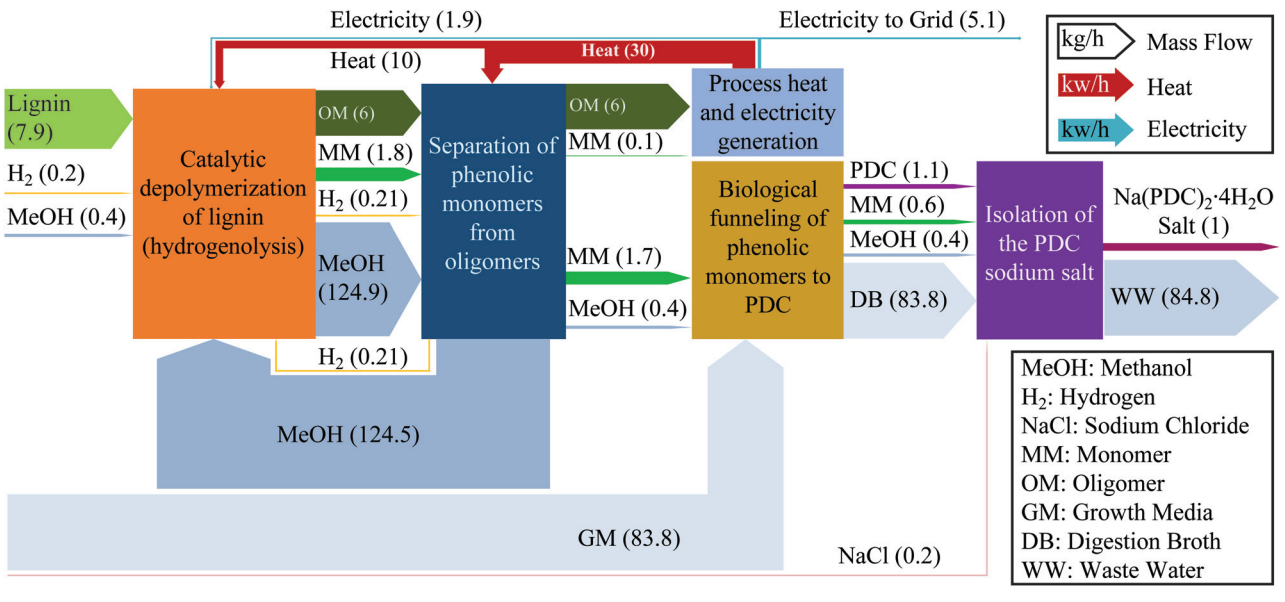

Fig. 4 Graphical representation of normalized mass and energy flows in the $Na(PDC)_2$ salt production process. The numbers in the parentheses represent the normalized mass flows (kg h^{-1}) or energy flows (kw h^{-1}) that are required throughout the process to make 1 kg of the product.

Table 4 Key data for plant design

Parameter	Conditions
Plant capacity	400 metric ton per day (16.7 metric ton per hour) of lignin
Lignin hydrogenolysis	
Reaction condition	200 °C, 65 bar, 2 h
Lignin : methanol : Hydrogen mass ratio	1 : 15.74 : 0.052
Catalyst (5 wt% Pd/C) : Lignin mass ratio	1 : 2
Catalyst lifetime	1 year
Lignin-to-monomer yield	23%
Biological funneling	
Reaction condition	30 °C, 1 atm, 50 h
Monomer-to-PDC yield	66%

Specifically, only the biomass fractionation and lignin recovery sections in Alonso *et al.*[24] were considered and the cost of the biomass fractionation was appropriately distributed among the outlets of the above sections based on their mass flows. The lignin unit cost was calculated as \$0.63 per kg. For comparison, Alonso *et al.* assumed a fixed lignin selling price of \$0.50 per kg in their analysis.[24]

In the proposed process pipeline, lignin, hydrogen, and methanol are fed into the hydrogenolysis system in the presence of the 5 wt% Pd/C catalyst. Five reactors, each with a volume of 228 m^3 and retention time equal to 2 hours, are used to produce monomers having a similar distribution of sidechains as reported in Table 2 in a 23% yield. Monomers are separated from oligomers, and the methanol and excess hydrogen are recycled. Recycled methanol and hydrogen streams mixed with the makeup amounts and fresh lignin are compressed and heated to the hydrogenolysis reactor conditions. The oligomer stream is sent to the boiler, whereas the monomer stream and growth media are fed into the bioreactor to produce PDC through microbial funneling. Glucose is included as the carbon source used by *N. aromaticivorans* strain PDC for growth. At this stage of analysis, the bioreactor section is simplified and does not consider other factors that influence the cost of reactor operation. The process models for monomer separation and solvent recovery were developed using the ASPEN PLUS process simulator (V10, Aspen Technology). A simplified mass and energy balance diagram is presented in Fig. 4. The overall calculated lignin-to-PDC yield (14 wt%) is similar to the experimental yields and was determined using a monomer-to-PDC yield of 66 wt%, a lignin-to-monomer conversion yield of 23%, and assuming minimal loss of aromatic monomers during separation. Product isolation from the bioreactor effluent is performed through Na$(PDC)_2$ salt precipitation with sodium chloride.[13,49] with the supernatant being sent for wastewater treatment. The calculated Na$(PDC)_2$ salt MSP, which is the price at which the total costs are equal to the revenues, is \$12.1 per kg Na$(PDC)_2$ salt (Fig. 5A). Under this scenario, the major cost contributor of the entire process is the cost of lignin (40% of the total cost of Na$(PDC)_2$ salt production), followed by biological funneling, which contributes 24% of the MSP (Fig. 5A). The hydrogenolysis process had a small contribution to the MSP (11%). However, Bartling *et al.*[50] recently reported on a technoeconomic analysis of an RCF process that considered the effect of reactor pressure and concluded that the capital cost of the RCF reactors is a major factor influencing the MSP of the product.[50] Indeed, when we modify the analysis to include pressure considerations, as in Bartling *et al.*, the calculated Na$(PDC)_2$ salt MSP increases by \$7.61 per kg, to \$19.71 per kg, and the hydrogenolysis section becomes the major contributor to the MSP, at 46%, followed by the lignin cost, at 25% (Fig. S8†).

The model estimates the total energy requirement of the process at 66 MW, which is approximately 39% of the heat generation in the boiler of the lignocellulosic biorefinery studied by NREL.[4] The process heat and electricity requirements can be met by combustion of the remaining lignin oligomer stream, and ~10.7 MW of excess electricity is available for sale to the grid. The largest heating requirements stem from monomer purification, which also recovers methanol, and for maintaining the temperature of the recycled methanol stream. Also, boiler capital and operating expenses contribute significantly (21%) to the cost of Na$(PDC)_2$ salt production (Fig. 5A). The efficiency of heat and electricity generation is assumed to be 80% and 54%, respectively.[4]

We performed a single-point sensitivity analysis, starting from the base-case parameter values reported in Table 4, to identify the parameters for which improvement will have significant impact on the process economics. Fig. 5B shows the reduction in the MSP (ΔMSP) compared to the base case when a single parameter is varied. This analysis indicates that the feedstock (lignin) is a significant cost contributor and that a 30% reduction in lignin cost would reduce the MSP by \$1.50 per kg. The methanol-to-lignin ratio has a relatively smaller impact, reducing the MSP by \$0.50 per kg (Fig. 5B); however, a 50% reduction in the methanol-to-lignin ratio could also reduce the total energy requirement by almost 49% because of the lower methanol quantities needed to be recovered and recycled. Note that, although the designed process is energy sufficient (base case), most biorefinery designs utilize the lignin as fuel for process energy, and rerouting some of the lignin to make bioproducts could make them energy deficient. Thus, a reduction in the methanol requirement would be beneficial to the overall integration. Increasing the lignin-to-monomer yield could also have a major impact in MSP, with a 50% increase in the current lignin-to-monomer yield decreasing the MSP by \$3.38 per kg. However, any further increase in monomer yield is coupled with a reduction in the quantity of oligomers that are used for heat and electricity generation, and therefore would make biorefinery operations dependent on purchasing energy form the grid.

The model predicts that another critical parameter is the monomer-to-growth media ratio, with a 50% increase (31.05 g L^{-1} *vs.* 20.7 g L^{-1} used in the base case) leading to a \$1.7 per kg reduction in the product MSP. We further studied the impact of this parameter because an increase in monomer-to-

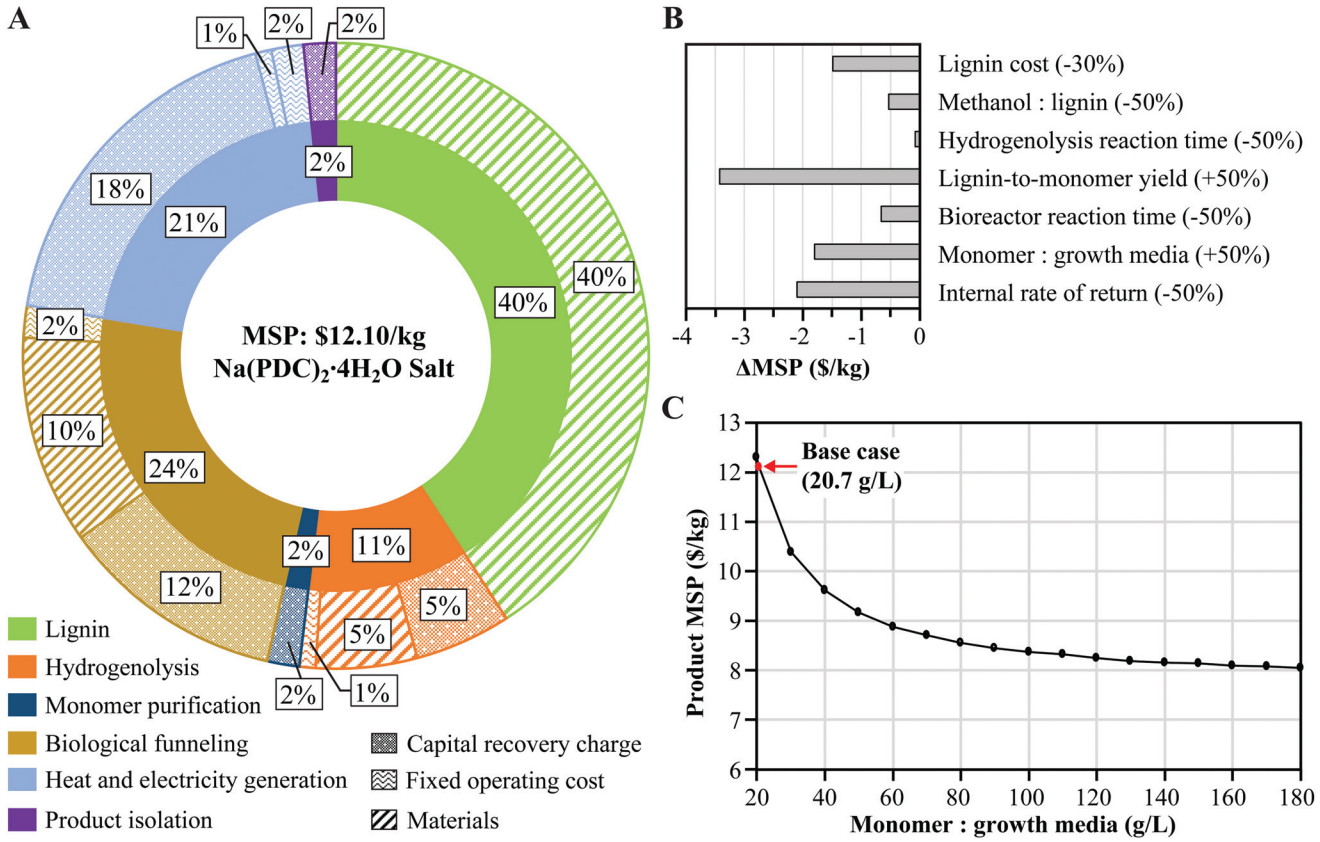

Fig. 5 (A) Cost contribution of each process section to the minimum selling price (MSP) of PDC, which is indicated in the center of the circles. The inner circle provides the cost contribution of each process section (lignin, hydrogenolysis, monomer purification, biological funneling, heat and electricity generation, and product isolation). The outer circle uses patterns to indicate the cost components (capital recovery charges, material costs, and fixed operating costs) within each of the process sections. The relative contribution of electricity is too small to be depicted in the figure. Process sections are differentiated using colors; (B) sensitivity analysis of design and cost parameters (ΔMSP indicates reduction from the base case MSP); (C) impact of monomer-to-growth media ratio on the product MSP (base case, 20.7 g L^{-1}, depicted using red marker).

growth media ratio leads to a reduction in the capital costs of the bioreactor and product isolation section, and an increase in the recovery of $Na(PDC)_2$, which depends on PDC solubility. As shown in Fig. 5C, increasing the monomer-to-growth media ratio to 130 g L^{-1} (from 20.7 g L^{-1} used in the base case) would result in a significant improvement, though a further increase has little effect on the MSP.

The residence times of the hydrogenolysis reactor and bioreactor had comparatively little impact on the process economics (Fig. 5B). This outcome changes when the analysis is performed considering hydrogenolysis reactor pressure (Fig. S8†), where hydrogenolysis becomes a major driver of the increased MSP, and reducing the hydrogenolysis retention time by 50% would reduce the MSP by 25% ($3.9 per kg). In addition, other factors that indirectly contribute to a smaller hydrogenolysis reactor, such as the methanol to lignin ratio and the lignin to monomer yield would have critical impacts on the MSP (Fig. S8†).

Finally, we also analyzed the impact of the internal rate of return (IRR). In the base case, we assumed an IRR equal to 30% to reflect the higher risk of investing in new technology, as used by Alonso *et al.*[24] As shown in Fig. 5B, a 50% decrease in the IRR, to 15%, results in an MSP reduction of $2.1 per kg. If a 10% IRR is used, as in NREL designs,[4] the MSP reduces by $2.7 per kg. The impact of IRR is also important in the analysis with the costlier reactor, for which a 50% decrease would reduce the MSP by $5.1 per kg.

Discussion

One approach to increase the value of lignin is to deconstruct it using chemical depolymerization methods that produce mixtures of aromatic compounds and subsequently funnel them into a single valuable product using engineered bacteria. Within a biorefinery context, approaches to obtain value from lignin should be compatible with obtaining value from the other polymers in plant biomass, such as cellulose and hemicelluloses. In this work, the lignin was extracted from plant biomass using GVL in a low-temperature process. When high-quality lignin and glucose are the desired products, the GVL process is implemented with two separate stages. The first

stage uses low temperature (here we used 90 °C for 90 min) to extract high-quality lignin and hemicellulose. The remaining biomass can be further processed to produce dissolving pulp (cellulose) that can be used in the manufacturing of textiles like Rayon.[23,24] Furthermore, when glucose is a desired final product, the remaining biomass is treated in a second stage with GVL at an increased temperature to perform acid catalyzed saccharification of the polysaccharides, which are depolymerized to monomers, dimers, and small oligomers. At these higher temperatures, some of the sugars start to dehydrate to form furfural and 5-hydroxymethylfurfural, and any lignin that was not extracted in the first stage and remained with the biomass pulp condenses considerably to produce a low-quality lignin that could be used to produce process heat and electricity. The process simulated in this study uses as the starting material the high-quality lignin obtained from the first stage of a two-stage GVL deconstruction process. Through this work we identified factors that impact the MSP of the Na $(PDC)_2$ salt produced. Below we discuss key observations from this analysis.

Biological funneling

Conversion feasibility of aromatic monomers

To make the hydrogenolysis product mixture compatible with biological funneling to PDC, we explored the feasibility of conversion of the major phenolic products known to result from catalytic hydrogenolysis under conditions that retain aromaticity of the products. Our results show that monoaromatics containing propanol (DSA and DCA), methyl (MS and MG), or carboxylic acid methyl ester (Me-D*p*CA, Me-DFA, and Me-*p*HBA) sidechains, can be metabolized into PDC with variable yields (Table 1). Methyl esters (Me-*p*HBA, Me-DH*p*CA, and Me-HDFA) were converted into PDC with near-stoichiometric yields, whereas aromatics with a propanol (DHSA and DHCA) or methyl sidechains (MS and MG) were converted at yields ranging from 28% to 66% (Table 1). The observation that these aromatics lead to PDC production predicts that they enter the central metabolic pathway for degradation of S-, G-, and H-type aromatic compounds in *N. aromaticivorans*.[9] Although enzymes that catalyze the initial steps in the degradation of aromatics with propanol, methyl, or methyl ester sidechains have not yet been identified, we predict that these aromatic compounds will first be transformed to syringic acid, vanillic acid, and *p*-hydroxybenzoic acids, which are the central intermediates, for S-, G- and H-type aromatic compounds, respectively (Fig. S9†). However, the less-than-stoichiometric PDC yield for some of these compounds also suggests that there may be alternative metabolic pathways for their degradation that would not have PDC as an intermediate metabolite. Such alternative pathways could lead to the diversion of a fraction of the aromatic substrate or result in accumulation of other byproducts, although we did not detect any extracellular product accumulation in cultures grown with these substrates. Indeed, we have recently identified an alternative pathway for syringic acid degradation and, when this pathway was blocked, we created a second generation *N. aromaticivorans* PDC strain that produces stoichiometric yields of PDC from S-type phenolic compounds.[51]

Compounds with a propyl (PS and PG) or ethyl sidechain (ES and EG), on the other hand, are converted to sidechain-oxidized products that accumulate in the medium without detectable accumulation of PDC. The propyl sidechains are oxidized to yield GPO and SPO (Fig. S2†). Similarly, the ethyl sidechain is oxidized to yield AS and AV (Fig. S4†). However, *N. aromaticivorans* is apparently unable to further catabolize any of these oxidized aromatics. Although we were able to select a catalyst that favored the production of aromatic monomers with propanol sidechains as the major product, the fraction of monomers with a propyl or ethyl sidechain was not insignificant, ranging from 13% to 21% in the different feedstocks tested (Table 2). Thus, the identification of these bottlenecks in the degradation of aromatic compounds by *N. aromaticivorans* creates opportunities to investigate further genetic modifications that would create different pathways for transformation of the propyl and ethyl aromatics, funneling them towards the central aromatic degradation pathways. For instance, the ability of *Rhodococcus rhodochrous* EP4 to grow on PG and EG has been recently reported, and enzymes that participate in the degradation of these alkylguaiacols have been identified,[52] providing enzyme targets for further *N. aromaticivorans* engineering.

Monoaromatic compounds without a sidechain (syringol and guaiacol) were completely (guaiacol) or partially (syringol) consumed but no PDC production was observed. Although metabolism of these compounds by *N. aromaticivorans* has not been investigated in detail, guaiacol metabolism *via* catechol has been studied in organisms such as *Pseudomonas putida* and this aromatic is used as a substrate for the production of muconic acid.[53] In addition, guaiacol and γ-hydroxypropiovanillone (HPV) are products of cleaving the β-*O*-4 interunit bond in the aromatic dimer guaiacylglycerol-β-guaiacyl ether (GGE), which has been extensively studied in *N. aromaticivorans*[54,55] and with cell-free *in vitro* enzymatic systems.[56] In *P. putida*, guaiacol is metabolized *via* a route that does not involve the production of PDC. We hypothesize that, in *N. aromaticivorans*, guaiacol may also be degraded *via* catechol (Fig. S9†).

Metabolism of syringol has been engineered into *P. putida* by heterologous expression of enzymes capable of *O*-demethylation of syringol.[57] As *N. aromaticivorans* only slowly metabolizes syringol (Fig. S1†), one possibility is that enzymes involved in the transformation of guaiacol may also have some activity with syringol. Independent of the enzymes involved, metabolism of syringol does not lead to PDC production by the engineered *N. aromaticivorans* strain (Fig. S9†).

Biological funneling of depolymerized lignin

For all biomass sources tested in this study, the engineered *N. aromaticivorans* PDC strain was able to produce PDC from deconstructed lignin showing the compatibility of this bacterium with the proposed valorization method. The efficiency of

producing PDC from the lignin hydrogenolysis products obtained *via* the GVL process was calculated to be greatest for poplar, followed by sorghum, maple, and switchgrass (Table 3). This trend was correlated to the yield of monomers from the respective depolymerized lignins (Fig. S10†). The chemical composition of the lignins positively correlates with the monomer yield to further increase PDC conversion efficiencies. Poplar lignin contains high levels of *p*HBA (0.5–3 wt% of the lignin),[58] whereas sorghum and switchgrass have significant quantities of *p*CA (10 wt% of the lignin).

In all cases, we note that the PDC yield was higher than predicted when the observed conversion yields of individual compounds were considered (Table 3). This observation can be explained by three different but not exclusive hypotheses. First, the conversion yields for some compounds in the mixtures of lignin depolymerized products could be higher than the yields observed in the single-compound experiments (Table 1). This is because the concentrations for lignin-derived aromatics in the microbial funneling experiments (Fig. 3 and Table S3†) were about 10 times lower than the concentrations used in the single-compound experiments (Fig. 2 and Fig. S1†). This concentration difference could affect the expression of alternative aromatic degradation pathways that do not involve the production of PDC as has been hypothesized for the degradation of the central aromatic metabolites 3-MGA and PCA in *N. aromaticivorans*.[9,51] Second, it is possible that the catalytic hydrogenolysis produces additional monomers that were not identified and quantified and that *N. aromaticivorans* strain PDC was able to convert into PDC. In fact, when the prediction of PDC yield is based in the assumption that all convertible monomers identified in the depolymerized lignin methanol solution are converted with stoichiometric yields (Table 3), the observed PDC yield is still higher for maple, sorghum, and switchgrass, although not for poplar. Third, it is possible that aromatic substrates other than monomeric compounds present in the depolymerized lignin mixture were converted into PDC. Previous studies have demonstrated that *N. aromaticivorans* can metabolize aromatic dimers, for example those interlinked *via* β-*O*-4 bonds.[54,55,59]

An important and novel outcome of this study is the demonstration that, for microbial funneling of lignin to products, the mixtures of aromatics produced by reductive lignin depolymerization are as good or better than the mixtures of aromatics produced from oxidative lignin depolymerization, at least with *N. aromaticivorans*. We previously reported a 59% PDC molar yield from solutions of oxidatively depolymerized lignin, from poplar, in which syringic acid, vanillic acid, *p*-hydroxybenzoic acid, and aromatic diketones were the main depolymerization products.[9] For comparison, the estimated PDC molar yield from the mixtures of reductively depolymerized poplar lignin in this study was 71% (Table 3). The molar yields were even higher with maple, sorghum, and switchgrass (Table 3).

Production of PDC has also been engineered in a *P. putida* strain that can convert vanillin and vanillic acid to PDC but cannot metabolize S-type aromatics.[16] Reported PDC yields from these substrates were stoichiometric when these G-type aromatics were extracted from Japanese cedar or birch[16] or from lignosulfonates,[17] and about 20% when the G-type aromatics were extracted from Kraft lignin.[16] For comparison, the reported PDC yields from vanillin and vanillic acid by *N. aromaticivorans* are 100% and 81%, respectively.[9] Besides having similarly high PDC yields from G-type aromatics, an advantage of PDC production by *N. aromaticivorans* compared to *P. putida* is therefore that *N. aromaticivorans* can produce PDC from the three types of phenolics compounds extracted from lignin (S-, G-, and H-type aromatics) as shown in this and an earlier study.[9]

Catalytic hydrogenolysis

As the screening for PDC production from different types of compounds formed by hydrogenolysis of lignins showed that only some of them (DSA, DCA, MS, MG, and the phenolic esters) are compatible with biological funneling using *N. aromaticivorans* strain PDC, the choice of catalyst (Pd/C,[29,34–36] Rh/C,[37] Ni/C,[35] and $NiAl_2O_3$ [33]) was limited to those that favor production of the propanol sidechain. We chose to use Pd/C from a commercially available source as this catalyst is a robust, commonly used, only slightly air and light sensitive unlike some other catalysts. We chose to use methanol as the solvent as it is fairly inexpensive, has a relatively low toxicity, and has been shown to produce mostly the propanol sidechain when used in combination with Pd/C, H_2 at 30 bar, and 200 °C.[20,28–32] The analysis of the crude filtered methanol product solution showed that, for all lignin sources we studied, the majority of the identified monomeric products were compounds that can be funneled into PDC, although a minor fraction of the products cannot be converted into PDC by the engineered *N. aromaticivorans* strain PDC (Table 1). Future efforts to improve the compatibility of catalytic hydrogenolysis with biological funneling by this or other engineered strains could focus on increasing product selectivity of the depolymerization process towards the phenolic compounds that can be funneled towards PDC production.

GVL extraction

The PDC yield per kg of lignin followed the order poplar > sorghum > maple > switchgrass (Table 3). However, when the efficiency of extracting lignin from each GVL-deconstructed biomass is considered, the ranking of PDC yields (per kg of WCW biomass) is poplar > switchgrass > sorghum > maple (Table 3). The lower PDC yield from maple can be explained by the lack of phenolic ester pendent groups on its lignin compared to the other biomass sources tested. Genetic modifications that increase the amount of ester pendent groups incorporated into lignin,[60–62] or introduce phenolates into plants that do not normally produce them,[61] could have a positive impact in the PDC yield from deconstructed biomass. As these yield values are strongly affected by the GVL extraction efficiencies (Table 2), improvements in lignin extraction can also have a significant impact in the overall PDC yield. A deconstruction approach that incorporates lignin depolymeri-

zation from WCW biomass such as reductive catalytic fractionation (RCF)[63] by lignin-first' approaches,[21] would allow the whole lignin fraction to be depolymerized without the losses from the pretreatment/extraction process.

Technoeconomic analysis

Our sensitivity analysis seeks to provide future research directions in developing technologies that will help in further reduction of the PDC production cost. To improve the economic prospect of microbial PDC production from biomass aromatics, future research could be aimed at (1) improving the monomer yield without increasing solvent requirement for the hydrogenolytic process, (2) finding a solvent that can improve or retain the monomer yields without operating at high pressures, (3) increasing the monomer-to-growth media ratio without increasing toxicity or impacting the PDC yield from the monomers, and (4) improving biomass deconstruction to reduce the lignin cost. Besides the large impact of the IRR used in the simulations, these are the factors that had the largest influence in the MSP of PDC in the sensitivity analyses (Fig. 5B and Fig. S8†) and that can be addressed with technological improvements.

For the base case simulation, we used a lignin to monomer yield of 23% (Table 3) which is comparable to the experimentally determined yield from poplar (20%) and higher than the yields from maple, sorghum, and switchgrass (Table 2). Thus, feedstock selection will be an important consideration when evaluating how to increase monomer yield. Selecting biomass that has elevated conversion efficiency, utilizing breeding or engineering to obtain plants with more ideal lignins, and increasing phenolate levels in plant cell walls are all strategies that can be used to enhance monomer yields, albeit they should not negatively affect the production of a carbohydrate-rich hydrolysate, which is a desired product within an integrated biorefinery. In addition, catalyst improvement can also increase monomer yields. We note that in this study the Pd/C catalyst was used as received, as the focus was not catalyst optimization to achieve the maximal yield possible, but to establish an estimated baseline cost of PDC production. Having determined which products of hydrogenolysis are compatible with PDC production by *N. aromaticivorans*, catalyst improvement research can now be guided towards maximizing production of monomers with propanol sidechains and minimizing production of monomers with propyl sidechains. Furthermore, the selection of solvent for the hydrogenolysis process is an important factor to consider, to reduce operating pressure in the hydrogenolysis reactor.[50]

The sensitivity analysis shows that the capital cost of the hydrogenolysis reactor is a factor to consider, but its effect on the MSP of PDC depends on the assumptions used regarding the material needed for the high-pressure hydrogenolysis reactor.[50] The size of the reactor is influenced by the hydrogenolysis reaction time, solvent choice (methanol in our case), and the solvent to lignin ratio, with the latter having a greater impact on the MSP according to the sensitivity analysis (Fig. 5B and Fig. S8†). The large amount of methanol that needs to be recycled is a significant cost driver of the process due to the energy intensive separation process simulated, which involves flash, heating, and distillation units (Fig. S7†). Bartling *et al.*[50] discussed alternative solvents that could be used in RCF to reduce reactor pressure and thus decrease capital cost, or the potential use of membranes to recover the solvent in a less energy intensive manner, both of which may be promising alternatives. From the point of view of connecting hydrogenolysis of lignin with microbial funneling, the choice of solvent cannot only consider the physical aspects of the process, but needs to take into account that not all the solvent can be recovered, and therefore, the microbial culture will be exposed to elevated solvent concentrations. *N. aromaticivorans* tolerates elevated methanol concentrations, but further exploration of the toxicity of other candidate solvents will need to be considered.

The monomer concentration in the base case scenario was set to 20.7 g L^{-1} (Fig. 5C), based on experimental evidence for concentrations of aromatic monomers that can sustain PDC production by *N. aromaticivorans* and considering that most of the methanol used during hydrogenolysis needs to be recovered and recycled. Increasing monomer delivery to the microbial culture may require evolution of PDC-producing strains that are more resistant to high concentrations of aromatics, microbial cultures with faster PDC production rates than currently available, or utilizing strategies to grow dense *N. aromaticivorans* cultures, such as membrane bioreactors.

The lignin cost was identified as another important driver of the MSP, suggesting that improvements in the biomass deconstruction process could also improve the economics of the proposed lignin to PDC process. In the sensitivity analysis, we kept the variation of lignin cost lower (−30%; Fig. 5B) than used for other parameters analyzed, recognizing that it may be difficult to reduce lignin cost by a large margin. In the simulations, lignin was obtained from a GVL deconstruction process similar to that described by Alonso *et al.*[24] As the two-stage GVL process uses low temperature to dissolve and extract the lignin and high temperature to process the carbohydrate pulp, the optimization of the low-temperature stage to improve lignin quality may reduce the yield of extracted lignin compared to scenarios in which it may be more desirable to have a more efficient process for carbohydrate polymer processing at the expense of lignin quality. As mentioned above, biomass deconstruction approaches that directly fractionate lignin from WCW biomass[21,50] are attractive alternatives to the purchasing of lignin from a biorefinery that uses GVL as the deconstruction process.

Energy self-sufficiency is another aspect to consider in a lignin to PDC process. In TEA models of biorefineries, some proposed approaches require auxiliary fuel (natural gas) and electricity (from the grid) as input to quench the energy demand of the integrated biorefinery,[64] or energy requirements are fulfilled by the use of hydrogen and natural gas.[65] Unlike the aforementioned systems, the lignin to PDC process simulated here is energetically sufficient even without using any additional energy streams that are available in the biore-

finery (*e.g.*, biogas from wastewater treatment). This is the result of using the fraction of lignin that is not recovered as monomers for heat and electricity generation (Fig. S7†). This underscores the concept that in an integrated biorefinery not all the lignin needs to be converted to a product such as PDC, as a major portion of the lignin may still be used to make the biorefinery energy self-sufficient.

Materials and methods

Chemicals

All commercially available chemicals were purchased from Sigma-Aldrich (St Louis, MO). PDC was produced and purified according to the procedure described in Perez *et al.*[9]

Biomass

The NM6 hybrid poplar (*Populus maximowiczii* × *nigra*) and hard maple (*Acer saccharum*) were debarked, chipped, dried, and fractionated to pass through a 5 mm round hole on a shaker table. The energy sorghum (*Sorghum bicolor*) and switchgrass (*Panicum virgatum*) were harvested with a John Deere 7350 Self-propelled forage harvester/chopper and dried.

Bacterial strains and culture conditions

The engineered strain of *N. aromaticivorans* DSM12444 (strain PDC) lacking the genes Saro_1879 (*sacB*), Saro_2819 (*ligI*), and Saro_2864/5 (*desC*/*desD*),[9] was used in this study. Cultures were grown in SMB media supplemented with the indicated carbon source at 30 °C. SMB media contains 20 mM Na_2HPO_4, 20 mM KH_2PO_4, 7.5 mM $(NH_4)_2SO_4$, 0.167 mM $ZnSO_4$, 0.125 mM $FeSO_4$, 0.028 mM $MnSO_4$, 0.006 mM $CuSO_4$, 0.009 mM $Co(NO_3)_2$, 0.016 mM $Na_2B_4O_7$, 24.319 mM $MgSO_4$, 1.667 mM $CaCl_2$, 0.013 mM $(NH_4)_6Mo_7O_{24}$. For routine culture and storage, the growth media were supplemented with 1 g L^{-1} glucose.

Bioconversion of individual compounds

N. aromaticivorans strain PDC cultures were grown in 10 mL of SMB media supplemented with 1 g L^{-1} glucose to reach stationary phase. The experiments were initiated by diluting the cultures with 10 mL of fresh SMB media supplemented with 2 g L^{-1} glucose and the corresponding aromatic compounds previously dissolved in methanol, to a concentration of 2 mM. The final concentration of methanol in the growth media was less than 0.5%. The cultures were grown in triplicate flasks, shaken at 200 rpm, and incubated at 30 °C for a total of 20 h. Bacterial cell density was monitored using a Klett-Summerson photoelectric colorimeter with a red filter. Samples were collected regularly, filtered through a 0.2 μm PES syringe filter and stored at −20 °C.

Lignin extraction

Lignin was extracted from ground biomass using the GVL pretreatment process.[23,66] Briefly, 185 g of biomass was mixed with 1665 g of a solvent system comprising 80 wt% GVL, 19 wt% water, and 100 mM sulfuric acid. In a typical run, this mixture was incubated at 90 °C for 90 min in a high-pressure reactor fitted with a custom-designed impeller system capable of mixing biomass at high solid concentration.[67] The resulting liquid was cooled to room temperature and the solid fraction was removed by filtration. The extracted lignin was precipitated by diluting the filtrate with water (1 : 9 v/v, filtrate : water). The suspension was left to settle for two days, then the lignin was pelleted by centrifugation and the supernatant decanted. The pellet was washed three times with boiling DI water, by suspending the solids and filtration. The wet solids were freeze-dried to obtain dry lignins that were used in the hydrogenolysis depolymerization without further purification.

Lignin hydrogenolysis

The lignin was treated by hydrogenolysis using hydrogen over palladium on a carbon (5 wt% Pd/C) catalyst in methanol. In a 50 mL Hastelloy Parr reactor, equipped with a mechanical stirrer and heating mantle, 750 mg of lignin, 375 mg Pd/C, 30 mL methanol, and 9 mg (65 nmol) 1,2-dimethoxybenzene (DMB, an internal standard for determining monomer yields) were added. The reactor was sealed, purged and pressurized with hydrogen gas to 30 bar. The reaction vessel was then heated to 200 °C at a ramp rate of 6 °C min^{-1} and held there for 3 h (200 °C, 65 bar). Then, the heating mantle was removed and the reactor was rapidly cooled back to room temperature using a compressed air stream to assist in cooling. Once at room temperature, the reaction vessel was slowly depressurized to minimize the loss of volatile product. The catalyst and any residual solids were removed by a 0.1 μm PTFE (polytetrafluoroethylene) filter. The product mixture, without removing the methanol, was stored at 5 °C until used. This mixture provided the same GC-FID-determined composition and PDC production from microbial digestion after >6 months storage in the freezer.

Analysis of aromatic hydrogenolysis monomers

Quantitative analysis of the aromatic monomers was performed on a Shimadzu GC-2010Plus equipped with an AOC-20i autosampler and a Phenomenex Xebron column (ZB-5HT 15 m × 0.25 mm × 0.25 μm), helium gas mobile phase held at a constant linear velocity of 35 cm s^{-1}, and hydrogen/compressed air FID gases. The injection port was set to 250 °C with a split ratio of 10 : 1. The temperature program was as follows: 50 °C for 0.5 min, then ramped to 100 °C at 20 °C min^{-1}, the ramped to 200 °C at 5 °C min^{-1}, the ramped to 305 °C at 30 °C min^{-1}, and held at 305 °C for 3 min. Calibration curves for the quantified monomers were determined by a seven point calibration curve relative to DMB. The calculated values were determined as: mmol mg^{-1} GVL-lignin relative to 100% recovery of 65 nmol DMB.

Depolymerized lignin bioconversion experiments

N. aromaticivorans strain PDC cultures were grown in 10 mL of SMB media supplemented with 6 mM glucose. The experiments were initiated by diluting the cultures with 10 mL of

fresh SMB media supplemented with 12 mM glucose and 20 mL L^{-1} methanol solution containing the products of lignin depolymerization. The cultures were grown in triplicate in flasks, shaken at 200 rpm, and incubated at 30 °C for 25 h. Bacterial cell density was monitored using a Klett-Summerson photoelectric colorimeter with a red filter. Samples were collected regularly, filtered with a 0.2 μm PES syringe filter and stored at −20 °C. Each of the three hydrogenolysis products obtained from each plant tissue was tested in three biological replicates.

Analysis of extracellular metabolites

Quantitative analysis of aromatic compounds and PDC was performed on a Shimadzu triple quadrupole liquid chromatography mass spectrometer (LC-MS, Nexera XR HPLC-8045 MS/MS). The mobile phase was a binary gradient consisting of solvent A (0.2% formic acid in water) and solvent B (methanol) at a flow rate of 0.4 mL min^{-1}. The column was conditioned at 5% B, the elution program was 5% B hold 0.1 min, ramp to 20% B at 0.5 min, ramp to 30% B at 3.5 min, ramp to 50% B at 5 min, ramp to 95% B at 5 min and hold for 1.5 min to wash the column, then reset the column by returning to 5% B at 7 min and holding for 2.5 min to equilibrate the column for the next injection. The stationary phase was a Kinetex F5 column (Phenomenex, 2.6 μm pore size, 2.1 mm ID, 150 mm length, P/N: 00F-4723-AN). All compounds were detected by multiple-reaction-monitoring (MRM) and quantified using the strongest MRM transition, Table S5.†

Quantitative analysis of glucose was performed on an Agilent 1260 infinity HPLC equipped with a refractive index detector (HPLC-RID) (Agilent Technologies, Inc., Palo Alto, CA) and an Aminex HPX-87H with Cation-H guard column (BioRad, Inc. Hercules, CA). The mobile phase was 0.01 M sulfuric acid at a flow rate of 0.5 mL min^{-1}.

PDC production process model

The proposed PDC productions process was modelled using Aspen Plus V.10 (Aspen Technology Inc., Massachusetts, USA) for a biorefinery processing capacity specified in NREL designs as 2000 metric ton per day of lignocellulosic biomass.[64,68] A simplified process flow diagram is depicted in Fig. 1 and the data used for the unit designs are provided in Table 1. The GVL-lignin stream produced as a product from the GVL-sugar stream biorefinery was set as 20 wt% of the biomass,[24] requiring the lignin conversion plant to process 400 metric ton per day of lignin. The lignin is subjected to hydrogenolysis (R1) as a 6% lignin loading in methanol under a 65 bar hydrogen atmosphere in the presence of 5 wt% Pd/C catalyst at 200 °C. Two reactors with volume of 600 m^3 are used in parallel, and the reactor volumes are designed to provide the reaction time of 2 h. The GVL-lignin is fragmented to phenolic monomers (23 wt%) and oligomers (77 wt%) by cleavage of β-aryl ether bonds and hydrolysis or transesterification of the lignin bound phenolic acids (*e.g.*, *p*CA, FA, and *p*HBA), as observed for poplar (Table 2). After the lignin is depolymerized by hydrogenolysis, the excess hydrogen (F1) and methanol (F2) are recovered, separated (F4) and recycled through a series of flash distillation tanks. The residual product mixture is then double distilled to recover the remaining methanol (F3 and DC). The phenolic monomers are also separated from the higher molecular weight oligomers and other products as part of the second distillation (DC). The high boiling oligomer stream is sent to a boiler for conversion into process heat and electricity. The phenolic monomer stream (primarily S/G-propanol and phenolic methyl esters) are fed alongside microbial growth media into a bioreactor (R2) for microbial funneling to PDC. The residence time in the bioreactor is 50 h. The parameters used for the design of hydrogenolysis reactor and bioreactor are presented in Table 4. After removal of the microbes, the PDC is precipitated with sodium chloride, filtered, and dried to produce the target product $Na(PDC)_2$ salt as a powder.[13,49]

Technoeconomic model

We assumed that the economics of PDC production are independent of any system converting sugars to fuels and that the raw materials and utilities are independently purchased. A discounted cash-flow analysis was performed based on the energy and mass balance obtained from the Aspen Plus simulations to calculate an MSP for the $Na(PDC)_2$ salt. The MSP provides an economic index to assess the pinch points in the GVL-lignin-to-PDC process *via* hydrogenolysis depolymerization of the monomers. The material and energy requirements to produce 1 kg $Na(PDC)_2$ salt are shown in Fig. 4A. The economic parameters and assumptions used for the techno-economic analysis are listed in Table S4 provided as a part of the ESI.†

Conclusions

In this study, we demonstrated the feasibility of integrating reductive chemical depolymerization of isolated lignin with conversion to a valuable product like PDC *via* biological funneling by an engineered strain of *N. aromaticivorans* (strain PDC). We also demonstrated that the strategy is technically feasible for lignin isolated from multiple biomass types and that the catalyst selection is important to create compatibility of reductive depolymerization with microbial funneling as *N. aromaticivorans* produces PDC from phenolics with propanol sidechains but not from phenolics with propyl sidechains. Catalyst selection may prove to be also important for compatibility with microbial funneling using other microorganisms. We identified key factors that impact the technical and economic feasibility of a biomass to PDC biorefinery. Further research is needed on the maximization of the carbon flow from lignin to PDC *via* increasing the convertible monoaromatic yield from lignin and broadening the substrate specificity of the microbial platform. It is also important to optimize the hydrogenolysis process to reduce the solvent to lignin ratio, since decreasing the amount of solvent needed has implications on reducing hydrogenolysis reactor size (capital cost) and the energy requirements during solvent recovery and

recycling. Finally, the biological conversion process should be improved targeting the maximization of the bioreactor productivity *via* increased substrate concentration in the reaction solution. We anticipate that improvements in these areas will positively impact other lignin-to-chemical strategies that utilize a variety of microbial platforms and products.

Author contributions

Jose M. Perez contributed to the conceptualization, data curation, formal analysis, investigation, visualization, and writing the original draft, and reviewing and editing; Canan Sener contributed to the conceptualization, data curation, formal analysis, investigation, writing the original draft, and reviewing and editing; Shamik Misra contributed to conceptualization, developing methodology, formal analysis, investigation, visualization, writing the original draft, and reviewing and editing; German E. Umana contributed to the investigation and data curation; Jason Coplien contributed to investigation and resources; Dennis Haak contributed to investigation and resources; Yanding Li contributed to the conceptualization of this work; Christos T. Maravelias contributed to conceptualization, developing methodology, reviewing and editing the original draft; Steven D. Karlen contributed to the conceptualization, data curation, formal analysis, visualization, supervision, writing the original draft, and reviewing and editing; John Ralph, contributed to conceptualization, supervision, writing, and reviewing and editing; Timothy J. Donohue contributed to conceptualization, supervision, writing, and reviewing and editing the original draft; Daniel R. Noguera contributed to conceptualization, supervision, writing, and reviewing and editing.

Conflicts of interest

There are no conflicts of interest to declare.

Acknowledgements

This work was supported by the U.S. Department of Energy (DOE) Great Lakes Bioenergy Research Center (DOE Office of Science BER grant no. DE-SC0018409). Additional funding from the Chilean National Commission for Scientific and Technological Research (CONICYT) as a fellowship to Jose M. Perez is also acknowledged.

References

1 A. J. Ragauskas, G. T. Beckham, M. J. Biddy, R. Chandra, F. Chen, M. F. Davis, B. H. Davison, R. A. Dixon, P. Gilna, M. Keller, P. Langan, A. K. Naskar, J. N. Saddler, T. J. Tschaplinski, G. A. Tuskan and C. E. Wyman, *Science*, 2014, **344**, 1246843.

2 J. Zakzeski, P. C. A. Bruijnincx, A. L. Jongerius and B. M. Weckhuysen, *Chem. Rev.*, 2010, **110**, 3552–3599.

3 M. V. Tsvetkov and E. A. Salganskii, *Russ. J. Appl. Chem.*, 2018, **91**, 1129–1136.

4 R. Davis, L. Tao, E. C. D. Tan, M. J. Biddy, G. T. Beckham, C. Scarlata, J. Jacobson, K. Cafferty, J. Ross, J. Lukas, D. Knorr and P. Schoen, Process design and economics for the conversion of lignocellulosic biomass to hydrocarbons: Dilute-acid and enzymatic deconstruction of biomass to sugars and biological conversion of sugars to hydrocarbons, Report NREL/TP-5100-60223, National Renewable Energy Laboratory (U.S.), Golden, CO (United States), 2013. https://www.nrel.gov/docs/fy14osti/60223.pdf.

5 A. Corona, M. J. Biddy, D. R. Vardon, M. Birkved, M. Z. Hauschild and G. T. Beckham, *Green Chem.*, 2018, **20**, 3857–3866.

6 R. Rinaldi, R. Jastrzebski, M. T. Clough, J. Ralph, M. Kennema, P. C. A. Bruijnincx and B. M. Weckhuysen, *Angew. Chem., Int. Ed.*, 2016, **55**, 8164–8215.

7 G. T. Beckham, C. W. Johnson, E. M. Karp, D. Salvachua and D. R. Vardon, *Curr. Opin. Biotechnol.*, 2016, **42**, 40–53.

8 J. H. Cecil, D. C. Garcia, R. J. Giannone and J. K. Michener, *Appl. Environ. Microbiol.*, 2018, **84**, 1–13.

9 J. M. Perez, W. S. Kontur, M. Alherech, J. Coplien, S. D. Karlen, S. S. Stahl, T. J. Donohue and D. R. Noguera, *Green Chem.*, 2019, **21**, 1340–1350.

10 E. Masai, S. Shinohara, H. Hara, S. Nishikawa, Y. Katayama and M. Fukuda, *J. Bacteriol.*, 1999, **181**, 55–62.

11 T. Michinobu, M. Hishida, M. Sato, Y. Katayama, E. Masai, M. Nakamura, Y. Otsuka, S. Ohara and K. Shigehara, *Polym. J.*, 2008, **40**, 68–75.

12 K. Shikinaka, Y. Otsuka, M. Nakamura, E. Masai and Y. Katayama, *J. Oleo Sci.*, 2018, **67**, 1059–1070.

13 M. Bito, Y. Otsuka, M. Nakamura, E. Masai, Y. Katayama, K. Shigehara and K. Shikinaka, *Waste Biomass Valorization*, 2019, **10**, 1261–1265.

14 Y. Otsuka, M. Nakamura, K. Shigehara, K. Sugimura, E. Masai, S. Ohara and Y. Katayama, *Appl. Microbiol. Biotechnol.*, 2006, **71**, 608–614.

15 C. W. Johnson, D. Salvachúa, N. A. Rorrer, B. A. Black, D. R. Vardon, P. C. St John, N. S. Cleveland, G. Dominick, J. R. Elmore, N. Grundl, P. Khanna, C. R. Martinez, W. E. Michener, D. J. Peterson, K. J. Ramirez, P. Singh, T. A. VanderWall, A. N. Wilson, X. Yi, M. J. Biddy, Y. J. Bomble, A. M. Guss and G. T. Beckham, *Joule*, 2019, **3**, 1523–1537.

16 Y. Qian, Y. Otsuka, T. Sonoki, B. Mukhopadhyay, M. Nakamura, J. Jellison and B. Goodell, *BioResources*, 2016, **11**, 6097–6109.

17 Y. Suzuki, Y. Okamura-Abe, M. Nakamura, Y. Otsuka, T. Araki, H. Otsuka, R. R. Navarro, N. Kamimura, E. Masai and Y. Katayama, *J. Biosci. Bioeng.*, 2020, **130**, 71–75.

18 M. Nakajima, Y. Nishino, M. Tamura, K. Mase, E. Masai, Y. Otsuka, M. Nakamura, K. Sato, M. Fukuda, K. Shigehara, S. Ohara, Y. Katayama and S. Kajita, *Metab. Eng.*, 2009, **11**, 213–220.

19 Z. Sun, B. Fridrich, A. de Santi, S. Elangovan and K. Barta, *Chem. Rev.*, 2018, **118**, 614–678.
20 W. Schutyser, T. Renders, S. Van den Bosch, S. F. Koelewijn, G. T. Beckham and B. F. Sels, *Chem. Soc. Rev.*, 2018, **47**, 852–908.
21 M. M. Abu-Omar, K. Barta, G. T. Beckham, J. S. Luterbacher, J. Ralph, R. Rinaldi, Y. Román-Leshkov, J. S. M. Samec, B. Sels and F. Wang, *Energy Environ. Sci.*, 2021, **14**, 262–292.
22 M. V. Galkin and J. S. M. Samec, *ChemSusChem*, 2016, **9**, 1544–1558.
23 J. S. Luterbacher, A. Azarpira, A. H. Motagamwala, F. Lu, J. Ralph and J. A. Dumesic, *Energy Environ. Sci.*, 2015, **8**, 2657–2663.
24 D. M. Alonso, S. H. Hakim, S. Zhou, W. Won, O. Hosseinaei, J. Tao, V. Garcia-Negron, A. H. Motagamwala, M. A. Mellmer, K. Huang, C. J. Houtman, N. Labbé, D. P. Harper, C. Maravelias, T. Runge and J. A. Dumesic, *Sci. Adv.*, 2017, **3**, e1603301.
25 J. S. Luterbacher, J. M. Rand, D. M. Alonso, J. Han, J. T. Youngquist, C. T. Maravelias, B. F. Pfleger and J. A. Dumesic, *Science*, 2014, **343**, 277–280.
26 E. E. Harris, J. D'Ianni and H. Adkins, *J. Am. Chem. Soc.*, 1938, **60**, 1467–1470.
27 J. Weitkamp, *ChemCatChem*, 2012, **4**, 292–306.
28 J. M. Pepper and Y. W. Lee, *Can. J. Chem.*, 1969, **47**, 723–727.
29 S. Van den Bosch, W. Schutyser, S.-F. Koelewijn, T. Renders, C. M. Courtin and B. F. Sels, *Chem. Commun.*, 2015, **51**, 13158–13161.
30 Y. Li, B. Demir, L. M. Vázquez Ramos, M. Chen, J. A. Dumesic and J. Ralph, *Green Chem.*, 2019, **21**, 3561–3572.
31 Y. Li, L. Shuai, H. Kim, A. H. Motagamwala, J. K. Mobley, F. Yue, Y. Tobimatsu, D. Havkin-Frenkel, F. Chen, R. A. Dixon, J. S. Luterbacher, J. A. Dumesic and J. Ralph, *Sci. Adv.*, 2018, **4**, eaau2968.
32 W. Lan, M. T. Amiri, C. M. Hunston and J. S. Luterbacher, *Angew. Chem., Int. Ed.*, 2018, **57**, 1356–1360.
33 S. Van den Bosch, T. Renders, S. Kennis, S. Koelewijn, G. Van den Bossche, T. Vangeel, A. Deneyer, D. Depuydt, C. Courtin, J. Thevelein, W. Schutyser and B. Sels, *Green Chem.*, 2017, **19**, 3313–3326.
34 K. M. Torr, D. J. van de Pas, E. Cazeils and I. D. Suckling, *Bioresour. Technol.*, 2011, **102**, 7608–7611.
35 T. Renders, S. Van den Bosch, T. Vangeel, T. Ennaert, S.-F. Koelewijn, G. Van den Bossche, C. M. Courtin, W. Schutyser and B. F. Sels, *ACS Sustainable Chem. Eng.*, 2016, **4**, 6894–6904.
36 W. Schutyser, S. Van den Bosch, T. Renders, T. De Boe, S.-F. Koelewijn, A. Dewaele, T. Ennaert, O. Verkinderen, B. Goderis, C. M. Courtin and B. F. Sels, *Green Chem.*, 2015, **17**, 5035–5045.
37 J. M. Pepper and P. Supathna, *Can. J. Chem.*, 1978, **56**, 899–902.
38 H. H. Nimz, D. Robert, O. Faix and M. Nemr, *Holzforschung*, 1981, **35**, 16–26.
39 D. C. C. Smith, *J. Chem. Soc.*, 1955, 2347–2351, DOI: 10.1039/JR9550002347.
40 F. Lu, S. D. Karlen, M. Regner, H. Kim, S. A. Ralph, R.-C. Sun, K. Kuroda, M. A. Augustin, R. Mawson, H. Sabarez, T. Singh, G. Jimenez-Monteon, S. Zakaria, S. Hill, P. J. Harris, W. Boerjan, C. G. Wilkerson, S. D. Mansfield and J. Ralph, *BioEnergy Res.*, 2015, **8**, 934–952.
41 J. J. Stewart, T. Akiyama, C. Chapple, J. Ralph and S. D. Mansfield, *Plant Physiol.*, 2009, **150**, 621–635.
42 K. Morreel, J. Ralph, H. Kim, F. Lu, G. Goeminne, S. Ralph, E. Messens and W. Boerjan, *Plant Physiol.*, 2004, **136**, 3537–3549.
43 F. Lu, J. Ralph, K. Morreel, E. Messens and W. Boerjan, *Org. Biomol. Chem.*, 2004, **2**, 2888–2890.
44 H. Kim, Q. Li, S. D. Karlen, R. A. Smith, R. Shi, J. Liu, C. Yang, S. Tunlaya-Anukit, J. P. Wang, H.-M. Chang, R. R. Sederoff, J. Ralph and V. L. Chiang, *ACS Sustainable Chem. Eng.*, 2020, **8**, 3644–3654.
45 A. Bhalla, N. Bansal, S. Pattathil, M. Li, W. Shen, C. A. Particka, S. D. Karlen, T. Phongpreecha, R. R. Semaan, E. Gonzales-Vigil, J. Ralph, S. D. Mansfield, S.-Y. Ding, D. B. Hodge and E. L. Hegg, *ACS Sustainable Chem. Eng.*, 2018, **6**, 2932–2941.
46 R. D. Hatfield, J. M. Marita, K. M. Frost, J. M. Grabber, J. Ralph, F. M. Lu and H. M. Kim, *Planta*, 2009, **229**, 1253–1267.
47 H. Kim and J. Ralph, *Org. Biomol. Chem.*, 2010, **8**, 576–591.
48 S. D. Mansfield, H. Kim, F. Lu and J. Ralph, *Nat. Protoc.*, 2012, **7**, 1579–1589.
49 T. Michinobu, M. Bito, Y. Yamada, Y. Katayama, K. Noguchi, E. Masai, M. Nakamura, S. Ohara and K. Shigehara, *Bull. Chem. Soc. Jpn.*, 2007, **80**, 2436–2442.
50 A. W. Bartling, M. L. Stone, R. J. Hanes, A. Bhatt, Y. Zhang, M. J. Biddy, R. Davis, J. S. Kruger, N. E. Thornburg, J. S. Luterbacher, R. Rinaldi, J. M. Samec, B. F. Sels, Y. Román-Leshkov and G. T. Beckham, *Energy Environ. Sci.*, 2021, **14**, 4147–4168.
51 J. M. Perez, W. S. Kontur, C. Gehl, D. M. Gille, Y. Ma, A. V. Niles, G. Umana, T. J. Donohue and D. R. Noguera, *Appl. Environ. Microbiol.*, 2021, **87**, e02794–e02720.
52 M. M. Fetherolf, D. J. Levy-Booth, L. E. Navas, J. Liu, J. C. Grigg, A. Wilson, R. Katahira, G. T. Beckham, W. W. Mohn and L. D. Eltis, *Proc. Natl. Acad. Sci. U. S. A.*, 2020, **17**, 25771–25778.
53 D. Vardon, M. A. Franden, C. Johnson, E. Karp, M. Guarnieri, J. Linger, M. Salm, T. Strathmann, G. Beckham and G. Ferguson, *Energy Environ. Sci.*, 2015, **8**, 617–628.
54 W. S. Kontur, C. A. Bingman, C. N. Olmsted, D. R. Wassarman, A. Ulbrich, D. L. Gall, R. W. Smith, L. M. Yusko, B. G. Fox, D. R. Noguera, J. J. Coon and T. J. Donohue, *J. Biol. Chem.*, 2018, **293**, 4955–4968.
55 W. S. Kontur, C. N. Olmsted, L. M. Yusko, A. V. Niles, K. A. Walters, E. T. Beebe, K. A. Vander Meulen,

S. D. Karlen, D. L. Gall, D. R. Noguera and T. J. Donohue, *J. Biol. Chem.*, 2019, **294**, 1877–1890.

56 D. L. Gall, W. S. Kontur, W. Lan, H. Kim, Y. Li, J. Ralph, T. J. Donohue and D. R. Noguera, *Appl. Environ. Microbiol.*, 2018, **84**, e02076-17.

57 M. M. Machovina, S. J. B. Mallinson, B. C. Knott, A. W. Meyers, M. Garcia-Borràs, L. Bu, J. E. Gado, A. Oliver, G. P. Schmidt, D. J. Hinchen, M. F. Crowley, C. W. Johnson, E. L. Neidle, C. M. Payne, K. N. Houk, G. T. Beckham, J. E. McGeehan and J. L. DuBois, *Proc. Natl. Acad. Sci. U. S. A.*, 2019, **116**, 13970–13976.

58 R. E. Goacher, Y. Mottiar and S. D. Mansfield, *Holzforschung*, 2021, **75**, 452–462.

59 D. L. Gall, J. Ralph, T. Donohue and D. Noguera, *Environ. Sci. Technol.*, 2014, **48**, 12454–12463.

60 S. Withers, F. Lu, H. Kim, Y. Zhu, J. Ralph and C. G. Wilkerson, *J. Biol. Chem.*, 2012, **287**, 8347–8355.

61 R. A. Smith, E. Gonzales-Vigil, S. D. Karlen, J.-Y. Park, F. Lu, C. G. Wilkerson, L. Samuels, J. Ralph and S. D. Mansfield, *Plant Physiol.*, 2015, **169**, 2292–3001.

62 D. L. Petrik, S. D. Karlen, C. L. Cass, D. Padmakshan, F. Lu, S. Liu, P. Le Bris, S. Antelme, N. Santoro, C. G. Wilkerson, R. Sibout, C. Lapierre, J. Ralph and J. C. Sedbrook, *Plant J.*, 2014, **77**, 713–726.

63 S. Van den Bosch, W. Schutyser, R. Vanholme, T. Driessen, S.-F. Koelewijn, T. Renders, B. De Meester, W. J. J. Huijgen, W. Dehaen, C. M. Courtin, B. Lagrain, W. Boerjan and B. F. Sels, *Energy Environ. Sci.*, 2015, **8**, 1748–1763.

64 R. Davis, N. Grundl, L. Tao, M. J. Biddy, E. C. D. Tan, G. T. Beckham, D. Humbird, D. N. Thompson and M. S. Roni, Process design and economics for the conversion of lignocellulosic biomass to hydrocarbon fuels and coproducts: 2018 biochemical design case update; biochemical deconstruction and conversion of biomass to fuels and products via integrated biorefinery pathways, Report NREL/TP-5100-71949, National Renewable Energy Laboratory (U.S.), Golden, CO (United States), 2018. https://www.nrel.gov/docs/fy19osti/71949.pdf.

65 Y. Liao, S.-F. Koelewijn, G. Van den Bossche, J. Van Aelst, S. Van den Bosch, T. Renders, K. Navare, T. Nicolai, K. Van Aelst, M. Maesen, H. Matsushima, J. M. Thevelein, K. Van Acker, B. Lagrain, D. Verboekend and B. F. Sels, *Science*, 2020, **367**, 1385–1390.

66 A. H. Motagamwala, W. Won, C. T. Maravelias and J. A. Dumesic, *Green Chem.*, 2016, **18**, 5756–5763.

67 D. J. Klingenberg, T. W. Root, S. Burlawar, C. T. Scott, K. J. Bourne, R. Gleisner, C. Houtman and V. Subramaniam, *Biomass Bioenergy*, 2017, **99**, 69–78.

68 D. Humbird, R. Davis, L. Tao, C. Kinchin, D. Hsu, A. Aden, P. Schoen, J. Lukas, B. Olthof, M. Worley, D. Sexton and D. Dudgeon, Process design and economics for biochemical conversion of lignocellulosic biomass to ethanol: Dilute-acid pretreatment and enzymatic hydrolysis of corn stover, Report NREL/TP-5100–47764, National Renewable Energy Laboratory (U.S.), Golden, CO (United States), 2011. https://www.nrel.gov/docs/fy11osti/47764.pdf.